Research article

Biomedical Chromatography

Received: 9 January 2016, Revised: 8 March 2016, Accepted: 11 March 2016 Published online in Wiley Online Library

(wileyonlinelibrary.com) DOI 10.1002/bmc.3721

An evaluation of the CYP2D6 and CYP3A4 inhibition potential of metoprolol metabolites and their contribution to drug–drug and drug–herb interaction by LC-ESI/MS/MS

Roshan M. Borkar[a,b], Murali Mohan Bhandi[a], Ajay P. Dubey[c], V. Ganga Reddy[b], Prashanth Komirishetty[d], Prajwal P. Nandekar[e], Abhay T. Sangamwar[e], Ahmed Kamal[b], Sanjay K. Banerjee[b,f]* and R. Srinivas[a,c]*

ABSTRACT: The aim of the present study was to evaluate the contribution of metabolites to drug–drug interaction and drug–herb interaction using the inhibition of CYP2D6 and CYP3A4 by metoprolol (MET) and its metabolites. The peak concentrations of unbound plasma concentration of MET, α-hydroxy metoprolol (HM), *O*-desmethyl metoprolol (ODM) and *N*-desisopropyl metoprolol (DIM) were 90.37 ± 2.69, 33.32 ± 1.92, 16.93 ± 1.70 and 7.96 ± 0.94 ng/mL, respectively. The metabolites identified, HM and ODM, had a ratio of metabolic area under the concentration–time curve (AUC) to parent AUC of ≥0.25 when either total or unbound concentration of metabolite was considered. *In vitro* CYP2D6 and CYP3A4 inhibition by MET, HM and ODM study revealed that MET, HM and ODM were not inhibitors of CYP3A4-catalyzed midazolam metabolism and CYP2D6-catalyzed dextromethorphan metabolism. However, DIM only met the criteria of >10% of the total drug related material and <25% of the parent using unbound concentrations. If CYP inhibition testing is solely based on metabolite exposure, DIM metabolite would probably not be considered. However, the present study has demonstrated that DIM contributes significantly to *in vitro* drug–drug interaction. Copyright © 2016 John Wiley & Sons, Ltd.

Additional supporting information may be found in the online version of this article at the publisher's web site.

Keywords: metoprolol metabolites; CYP2D6; CYP3A4; drug–drug interaction

Introduction

It is common in the treatment of patients for multiple drugs to be co-administered, and patients often consume herbal supplements along with prescribed medicines (Chavez *et al*., 2006; Dunning, 2003; Peng *et al*., 2004). As a consequence, there is a risk of drug–drug interactions (DDIs; Edwards and Aronson, 2000) and drug–herb interaction (DHIs; Pal and Mitra, 2006). DDIs or DHIs include induction and inhibition of metabolizing enzymes and drug efflux proteins (Pal and Mitra, 2006). They can result in a significant increase in the systemic exposure (area under curve, AUC) through altered drug absorption, metabolism and distribution, leading to toxicity (Sproule *et al*., 1997; Patsalos and Perucca, 2003).This issue cannot be understated, as it may lead to serious adverse drug reactions.Therefore, the US Food and Drug Administration (2012) (FDA) and the European Medicines Agency (2012) (EMA) recommend methods for performing pre-clinical risk assessment and quantitative DDI. Guidelines suggest that potential enzyme inhibitory effects of phase I metabolites should be considered in DDI risk assessment if metabolite AUC is >25% of

* Correspondence to: R. Srinivas, National Centre for Mass Spectrometry, CSIR-Indian Institute of Chemical Technology, Hyderabad, 500 007, India. Email: srini@iict.res.in

S. K. Banerjee, Medicinal Chemistry and Pharmacology Division, CSIR-Indian Institute of Chemical Technology, Hyderabad, 500 007, India. Email: banerjees74@hotmail.com

[a] National Centre for Mass Spectrometry, CSIR-Indian Institute of Chemical Technology, Hyderabad 500 007, India

[b] Medicinal Chemistry and Pharmacology Division, CSIR-Indian Institute of Chemical Technology, Hyderabad 500 007, India

[c] Department of Pharmaceutical Analysis, National Institute of Pharmaceutical Education and Research, Balanagar, Hyderabad 500037, India

[d] Department of Pharmacology and Toxicology, National Institute of Pharmaceutical Education and Research, Balanagar, Hyderabad 500037, India

[e] Department of Pharmacoinformatics, National Institute of Pharmaceutical Education and Research, Sector 67, S.A.S. Nagar (Mohali)160 062 Punjab, India

[f] Drug Discovery Research Center, Translational Health Science and Technology Institute, Faridabad 121001, India

Abbreviations used: DDI, drug–drug interaction; DHI, drug–herb interaction; DIM, desisopropyl metoprolol; EIC, extracted ion chromatogram; ESI, electrospray ionization; HLMs, human liver microsomes; HM, α-hydroxy metoprolol; IICT, Indian Institute of Chemical Technology; MET, metoprolol; NADPH, β-nicotinamide adenine dinucleotide phosphate; ODM, *O*-desmethyl metoprolol; PAPS, adenosine 3′-phosphate 5′-phosphosulfate; RED, rapid equilibrium dialysis; RLMs, rat liver microsomes; TBME, *tert*-butyl methyl ether; UDPGA, uridine 5′-diphosphoglucuronic acid trisodium salt.

the parent AUC ($AUC_m/AUC_p \geq 0.25$). The EMA further emphasizes the need to investigate the enzyme inhibitory potential of phase I metabolites with AUC >10% of the drug-related exposure if protein binding is available. Metabolites may constitute a risk factor for drug toxicity. In line with this, the FDA and EMA issued Metabolites in Safety Testing (MIST) and International Conference on Harmonization M3 guidelines (ICH-M3), respectively. MIST emphasizes metabolites that circulate in concentrations >10% of the parent drug concentration at steady state while ICH-M3 focuses on metabolites that circulate at 10% of total drug-related material. However, both guidelines focus on toxicity testing but not on the inhibitory potential of metabolites on cytochrome P450 (CYP) enzymes.

CYP enzymes such as CYP1A2, CYP2C9, CYP2C19, CYP2D6 and CYP3A4 are responsible for the majority of drug metabolism. Among these, CYP3A4, CYP2C9, CYP2C19 and CYP2D6 are the major enzymes, involved in 80% of phase I drug metabolisms. However, drugs undergo CYP metabolism other than that involved in CYP inhibition. Inhibition of CYP enzymes by other co-administred drug has led to the removal of several drugs from the market (Lasser *et al*., 2002). In order to ensure patient safety, FDA and EMA guidelines suggest *in vitro* metabolic studies to determine the substrate and inhibition properties of CYP of new chemical entities in early drug discovery. However, it has been recognized that inclusion of many major circulating metabolites in DDI or DHIs prevents false negative predictions (Yeung *et al*., 2011). There have been few studies in the literature on the importance of metabolites in DDIs and DHIs and their interaction with CYP enzymes. The CYP inhibition properties of metabolites are not well characterized in clinical DDIs. Hence, more studies are required to evaluate the role of major circulating metabolites in inhibitions of CYP and their contribution towards DDIs and DHIs.

Metoprolol (MET), a selective β1-receptor blocker, is metabolized by CYP2D6 to form α-hydroxy metoprolol (HM) and *O*-desmethyl metoprolol (ODM). ODM is further metabolized to form MET acid. Recent studies suggest the involvement of CYP3A isozymes in the *O*-demethylation pathway in rats (Boralli *et al*., 2009) and humans (Cerqueira *et al*., 2005). Multiple dose administration of MET showed increased plasma concentration of MET when compared with single-dose treatment (Kendall *et al*., 1980). This may be associated with a change in the bioavailability and oral clearance of the drug. Scott *et al*. (1991) reported that MET increased the AUC of bromozepam by 35%. It is not known whether MET and its major metabolites inhibit any CYP enzymes. It may be possible that metabolites of MET contribute to CYP inhibition, and involvement of MET metabolites in DDI risk assessment may change the risk categorization of the metabolites significantly. Also DDIs involving MET are not characterized and further investigations are required to determine the potential contribution of the other major MET metabolites to *in vivo* CYP2D6 and CYP3A4 interaction.

Therefore, the aim of the present study was to systematically evaluate the contribution of MET and its metabolites in the inhibition of CYP2D6 and CYP3A4 after MET administration to rats. The circulating metabolites of MET were observed in the plasma following an administration of 2 mg/kg dose of MET to rats. The concentrations of the metabolites that reached the recommended plasma cutoff (FDA and EMA guideline) were further used for the *in vitro* inhibition potential for CYP2D6 and CYP3A4. However it is unclear regarding the role of minor metabolites in DDI risk assessment. Owing to uncertainty, *in vitro* and *in vivo* (plasma, urine and feces) major and minor metabolites were identified and characterized by LC/ESI/MS/MS. Furthermore, metabolites were evaluated for DDI risk assessment by *in silico* and *in vitro* assay.

Material and methods

Chemicals and regents

The working standard of MET was a gift from the National Institute of Pharmaceutical Education and Research (NIPER), Hyderabad, India. α-Hydroxy metoprolol and ODM were purchased from Santa Cruz Biotechnology Inc., Texas, USA. HPLC-grade acetonitrile and methanol were purchased from Merck (Mumbai, India) and used without further purification. Water was purified using a Millipore Milli-Q plus purification system (Millipore Corp., Bedford, MA, USA). Ammonium bicarbonate and sodium hydroxide were purchased from Sigma-Aldrich Co., St Louis, MO, USA. Dichloromethane was purchased from Merck. 4-(2-Methoxyethyl)-phenol was purchased from TCI Chemicals, Japan. All other chemicals used in the method were of analytical grade. β-Glucuronidase from *Helix pomatia*, β-nicotinamide adenine dinucleotide phosphate (NADPH), reduced tetra (cyclohexylammonium) salt, warfarin, human liver microsomes (HLMs), human liver S9 fraction, uridine 5′-diphosphoglucuronic acid trisodium salt (UDPGA) and adenosine 3′-phosphate 5′-phosphosulfate (PAPS) were purchased from Sigma-Aldrich. Tacrine, diclofenac, dextromethorphan, midazolam, *S*-mephenytoin, ketoconazole, sulfafenazole, *N*-3-benzylnirvanol, quinidine and α-naphthoflavone were procured from NIPER, Hyderabad, India.

Instrumentation

Analysis was carried out on a U-HPLC instrument (Thermo Scientific Accela™, Thermo Fisher Scientific, San Jose, CA, USA) equipped with a quaternary pump, a de-gasser, a diode-array detector, an autosampler and a column compartment. Mass spectrometric analysis was carried out on an Orbitrap high-resolution mass spectrometer (Exactive™, Thermo Fisher Scientific, Bremen, Germany) equipped with a heated electrospray ionization (ESI) source and used for HRMS analysis. The data acquisition was under the control of Xcalibur software. The extracted ion chromatograms (EICs) were generated by extracting a small range (e.g. ±5–10 ppm) centered on the exact *m/z* of each analyte. For MS/MS experiments, a quadrupole–time of flight mass spectrometer (Q-TOF/MS; Agilent Technologies, 6540 series, USA) equipped with an ESI source was used. The data acquisition was performed under the control of Mass Hunter workstation software.

Equilibrium dialysis was performed using rapid equilibrium dialysis (RED) device, Pierce Biotechnology, Thermo Scientific (Rockford, IL USA). The RED device consists of a single-use base plate made from Teflon and the inserts. Each insert comprises two side-by-side chambers separated by an O-ring-sealed vertical cylinder of dialysis membrane (molecular weight cut-off 8000 kDa). Assay incubation was done in the Thermomixer (Eppendorf, Hamburg, Germany). Evaporation of samples was done on a ScanVac speed vacuum concentrator (*mas-tek* Instruments Co., Hyderabad, India).

Animals

All animal experiments were undertaken with the approval of Institutional Animal Ethical Committee of Indian Institute of Chemical Technology (IICT), Hyderabad. Female Sprague–Dawley rats (200–250 g) were purchased from the Teena Biolab, Hyderabad, India. The animals were housed in BIOSAFE, the animal quarantine

facility of IICT, Hyderabad, India. The animal house was maintained at temperature 22 ± 2 °C with relative humidity of 50 ± 15% and a 12 h dark/light cycle. The animals were fasted for 12 h prior to pharmacokinetic study. Six female Sprague–Dawley rats with similar weight and age were utilized to carry out the present pharmacokinetic study to reduce the variation in drug concentration in plasma.

Molecular docking studies

Molecular docking of HM, ODM, metoprolol acid and *N*-desisopropyl metoprolol (DIM) and quinidine to CYP2D6 was performed using the three-dimensional crystal structure of substrate-free CYP2D6 (PDB code 2F9Q) obtained from the protein data bank, solved at 3.00 Å resolution (Rowland *et al*., 2006). Similarly, molecular docking of MET metabolites and ketoconazole to CYP3A4 (PDB ID 1TQN for CYP3A4, solved at 2.05 Å resolution; Yano *et al*., 2004) was performed using the Glide molecular docking program included in Schrodinger suite 9.0.02 (Friesner *et al*., 2004). The three-dimensional structures of proteins were prepared using the Protein Preparation Wizard included in Schrodinger suite 9.0.02. The centroid of the co-crystallized ligand was used for protein active site grid definition with a grid size of 30 Å. The previously validated molecular docking parameters were used for the docking exercise (Nandekar *et al*., 2013). Molecular docking was performed with precision using OPLS (2005) Forcefield (Kaminski *et al*., 2001). Scaling factor of 0.8 with partial cut-off of 0.25 was used. The best-docked structure for each ligand was selected on the basis of Glide docking score.

Identification and characterization of *in vitro* and *in vivo* MET metabolites

Preparation of microsomes

Preparation of liver microsomes. The liver microsomes were prepared, as per the literature (Schenkman and Cinti, 1978) but with slight modification (see the Supporting Information). Protein concentration of RLM samples was determined by the Bradford method using bovine serum albumin as the standard and it was 8.02 μg/μL.

Preparation of intestine microsomes. A literature method was employed to prepare intestinal microsomes (Cotreau *et al*., 2000; Takemoto *et al*., 2003) with slight modification (see the Supporting Information). The protein concentration of intestinal microsomes samples was determined by Bradford method using bovine serum albumin as the standard and it was 2.47 μg/μL.

Preparation of heart microsomes. The heart microsomes were prepared by slight modification of the method proposed by Barakat *et al*. (2001) (see the Supporting Information). The protein concentration of heart microsomes samples was determined by Bradford method using bovine serum albumin as the standard and it was 12.58 μg/μL.

In vitro phase I metabolite studies

For *in vitro* phase I metabolism study, 1 μM MET was incubated to the standard preincubation mixture (final volume, 330 μL) consisting of rat liver microsomes/rat intestinal microsomes/rat heart microsomes/human liver microsomes (0.28 mg/mL protein concentration) and 100 mM phosphate buffer solution (pH 7.4). The mixture was pre-incubated for 10 min at 37 °C. A 2.5 mM cofactor was added and incubated for 60 min at 37 °C to prepare the incubation mixture. Blank samples without cofactor and zero minute samples with cofactor were prepared. Midazolam is considered as positive control sample and 1-hydroxy midazolam is characterized. The reaction was terminated by adding ice-cold acetonitrile containing 10 ng/mL concentration of IS followed by 200 μL of 0.1% sodium hydroxide. This mixture was thoroughly mixed and 800 μL of *tert*-butyl methyl ether (TBME) and dichloromethane (1:1) was added. The mixture solutions were kept in a shaker for 10 min and then supernatant layer was taken into another Eppendorf tube. Evaporation of supernatant was done on ScanVac speed vacuum concentrator and 100 μL of methanol was added. Only 10 μL aliquots of sample solution were injected into the UPLC/HRMS system for analysis.

In vitro phase II metabolite studies

Incubation of MET in S9 fraction was performed at 10 μM in duplicate. The S9 fraction (3.33 mg/mL protein concentration) was prepared in 100 mM potassium buffer solution (pH 7.4). The mixture was preincubated at 37 °C for 10 min prior to the reaction. To initiate the reaction, cofactor UDPGA (2 mM), NADPH (1 mM), PAPS (1 mM) and alamethicin (25 μg/mL) were added to give a 330 μL final volume. Blank incubations were performed without cofactors. Moxifloxacin is considered as positive control sample and glucuronide and sulfate conjugate of moxifloxacin were characterized. The reaction mixture was incubated for 60 min and terminated by adding 200 μL of ice cold acetonitrile containing 20 ng/mLof IS. Only 10 μL aliquots of final reaction solution were injected into UPLC/ESI/HRMS system for the determination of conjugated metabolites of MET.

In vivo metabolite studies

For *in vivo* metabolite generation, three adult female Sprague–Dawley rats were kept in metabolic cages for urine and feces collection. These were acclimatized for 2 h before dosing. The animals were dosed similarly; blood, urine and feces samples were collected before dosing and 0–2, 2–4, 4–6, 6–8, 8–10 and 10–12 h post-dose. The samples from blood, urine and feces were pooled together to generate a single sample of each matrix and stored at −20 °C until analysis. Samples were prepared according to the optimized extraction technique (Raju *et al*., 2012).

For *in vivo* phase II study, an aliquot of each plasma and urine samples collected after dosing 2 mg/kg of MET to rats was treated with β-glucuronidase from *Helix pomatia* containing some companion sulfatase to establish the importance of conjugation reactions in the elimination of MET. To an aliquot of 50 μL plasma, 30 μL of β-glucuronidase and 420 μL of Tris–HCl buffer (50 mM, pH 7.4) were added and incubated for 2 h at 37 °C. After incubation, the samples were centrifuged at 20,000 ***g*** at 4 °C for 10 min. To the supernatant, 5 μL of 50 ng/mLof IS and 200 μL of 0.1% sodium hydroxide were added. This mixture was thoroughly mixed and 800 μL of TBME and dichloromethane (1:1) was added. Evaporation of supernatant was done on a ScanVac speed vacuum concentrator and 100 μL of methanol was added. MET, HM and ODM were measured using the UPLC/ESI/HRMS system as described below. The quantification of the conjugates in plasma was determined by subtracting the concentrations of each analyte in control plasma from concentrations of the analytes in β-glucuronidase treated plasma.

UPLC-MS/Q-TOF analysis

In silico metabolites of metoprolol were predicated using MetaSite ™ from Molecular Discovery (Middlesex, UK). To elucidate the structures of the metabolites, the fragmentation of the $[M+H]^+$ ions of MET and its metabolites was examined using UPLC-MS/Q-TOF experiments in combination with accurate mass measurements. The separation of MET and its metabolites was achieved by using Waters acquity C_{18} column (50 × 2.1 mm i.d.; particle size 1.7 μm, Waters Corporation, Milford, MA, USA) and mobile phase consisting of a mixture of 10 mM ammonium bicarbonate (A)–methanol (B) in gradient elution mode. The gradient solvent program was set as follows [time (min)/% proportion of solvent B]: 0–05/80; 005–3/60; 3–5/80; and 5–10/80. The flow rate of the mobile phase was 0.15 mL/min, the column temperature 25 °C and the injection volume 10 μL. For MS/MS experiments of MET and its metabolites, typical operating source conditions for MS scan in positive ESI mode were optimized as follows: the fragmentor voltage was set at 144 V; the capillary at 3500 V; and the skimmer at 65 V. Nitrogen was used as the drying (325 °C,10 L/min) and nebulizing (40 psi) gas. For collision-induced dissociation experiments, keeping MS1 static, the precursor ion of interest was selected using the quadrupole analyzer and the product ions were analyzed using a TOF analyzer. Ultra-high-purity nitrogen gas was used as collision gas. All the spectra were recorded under identical experimental conditions and were an average of 20–25 scans. The product ions of all the protonated metabolites were compared with the product ions of protonated MET, to assign likely structures for the observed metabolites. The elemental compositions of protonated metabolites and their fragment ions have been confirmed by accurate mass measurements.

Synthesis of *N*-desisopropyl metoprolol metabolite

A description of synthesis procedure of DIM metabolite is given in the Supporting Information (Pujala *et al*., 2011; Zhang *et al*., 2008). The *Clog*P value of DIM was 0.32 and it is less lipophilic than MET.

^{1}H NMR (400 MHz, $CDCl_3$): 7.13 (d, J = 8.55 Hz, 2H), 6.84 (d, J = 8.55 Hz, 2H), 4.1 (m, 1H), 3.97 (d, J = 4.64, 2H), 3.56 (t, J = 7.09, 2H), 3.35(t, 3H), 2.80–2.92(m, 4H), 2.33(bs, 2H) (Fig. S1 in the Supporting Information); MS (ESI): m/z 226 $[M+H]^+$. HRMS (ESI) calculated for $C_{12}H_{20}NO_3$ $[M+H]^+$ 226.14286; observed: 537.14377, error −4.02 ppm.

Quantification of metoprolol and its metabolites in rat plasma

Preparation of stock, working solutions and internal standard

The stock solution of MET, HM, ODM and DIM were prepared in methanol–water (1:1). Serial dilutions were made to prepare the primary aliquots of MET, HM, ODM and DIM in methanol–water (1:1) for calibration curve and quality control (QC) samples. Similarly, stock solution of 1 mg/mL of atenolol (internal standard, IS) was also prepared in methanol–water (1:1), further diluted to prepare working solution containing a concentration of 10 ng/mL.

Preparation of calibration and QC samples

A primary aliquot of 5 μL of MET was spiked in 90 μL of blank K-3 EDTA rat plasma to yield calibration curve samples ranging from 0.5 to 200 ng/mL. Similarly, HM, ODM and DIM were spiked in plasma to yield calibration curve samples in the ranges 0.5–200, 1–200 and 1–200 ng/mL, respectively. Low, middle and high QC samples (LQC, MQC and HQC) at three different levels were prepared independently at concentrations of 1.5 ng/mL (LQC), 100 ng/mL (MQC) and 200 ng/mL (HQC) for MET and HM, whereas a concentration of 2.0 ng/mL (LQC) was used for ODM and DIM. Similarly, quality control samples (20, 100, 200 ng/mL) were also prepared. Blank plasma sample and zero samples were also prepared and analyzed. For liver tissues 5 μL of the primary aliquot of MET was spiked in 90 μL of pre-homogenized blank liver tissue in phosphate buffer solution (pH 7.4; 100 mg/mL of tissues) to yield calibration curve samples ranging from 1 to 200 ng/mL. Similarly, quality control samples (20, 100 and 200 ng/mL) were prepared. Blank plasma sample, tissues sample and zero samples were also prepared and analyzed. All the stock solutions were stored at 0–4 °C for further use.

Extraction of MET, HM, ODM and DIM from plasma

To an aliquot of 100 μL of plasma sample and liver tissue for calibration standard and test samples, 5 μL of IS solution was added at a concentration of 10 ng/mL, followed by 200 μL of 0.1% sodium hydroxide. This mixture was thoroughly mixed and 800 μL of TBME and dichloromethane (1:1) was added. The mixture solutions were kept in shaker for 10 min and then a supernatant layer was taken into another Eppendorf tube. Evaporation of supernatant was done on a ScanVac speed vacuum concentrator and 100 μL methanol was added. Only 10 μL aliquots of sample solution were injected into UPLC/MS system for analysis.

UPLC/ESI/HRMS

The separation of MET, HM, ODM and DIM was achieved using Waters acquity C_{18} column (50 × 2.1 mm i.d.; particle size 1.7 μm, Waters Corporation, Milford, MA, USA) and mobile phase consisting of a mixture of 10 mM ammonium bicarbonate (A)–methanol (B) in a gradient elution mode. The gradient solvent program was set as follows [time (min)/% proportion of solvent B]: 0–05/80; 05–2/60; 2–4/80; 4–6/80. The flow rate of the mobile phase was 0.15 mL/min, the column temperature 25 °C and the injection volume 10 μL. Substrate dependent parameters and instrumental parameters were optimized by infusing clear solutions of MET, HM, ODM, DIM and the atenolol (IS) separately using a syringe pump. The typical operating source conditions for MS scan in positive ion ESI mode were optimized as follows: sheath gas flow rate, 15; auxiliary gas flow rate, 3; spray voltage, 3.50 kV; capillary temperature, 300 °C; capillary voltage, 30.00 V; tube lens voltage, 80.0 V; skimmer voltage, 24.00 V; and heater temperature, 250 °C. The theoretical monoisotopic m/z of each $[M+H]^+$ was derived from the elemental composition. The full-scan mode in the mass range m/z 250–350 includes MET, HM, ODM and IS and EICs (m/z theoretical ± 5 ppm). For quantification, EICs of $[M+H]^+$ at m/z 268.19132, 284.18629, 254.17574, 226.14377 and 267.17072 for MET, HM, ODM, DIM and atenolol with a 5 ppm range centered on the exact m/z values were generated, respectively (Fig. 1). Representative chromatograms of blank plasma, blank plasma spiked with IS, blank plasma spiked with MET and rat plasma samples are shown in Fig. 2. The

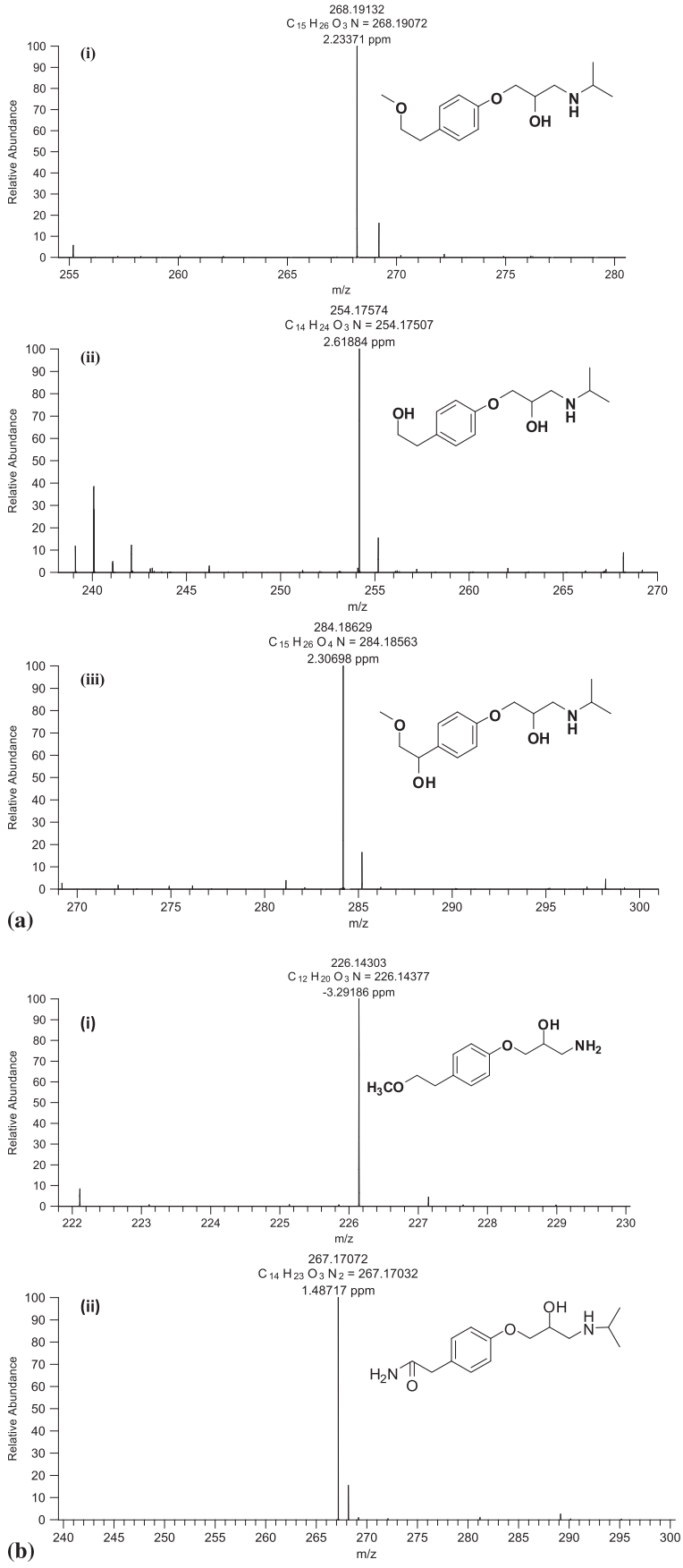

Figure 1. (a) Positive ion ESI-HRMS spectra of (i) metoprolol (*m/z* 268.19132), (ii) desmethyl metoprolol (*m/z* 254.17502) and (iii) α-hydroxy metoprolol (*m/z* 284.18629). (b) Positive ion ESI-HRMS spectra of (i) *N*-desisopropyl metoprolol (*m/z* 226.14377) and (ii) atenolol (*m/z* 267.17072).

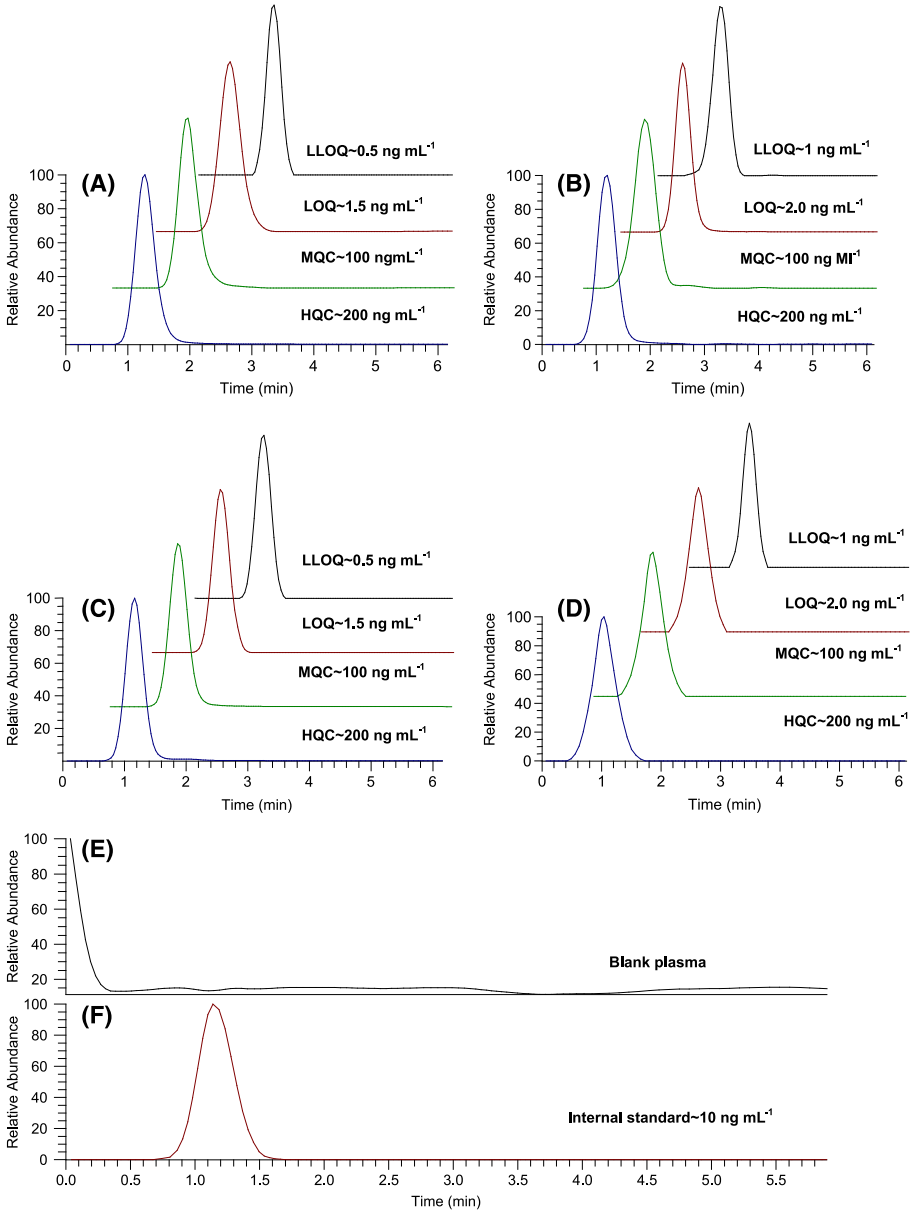

Figure 2. Extracted ion chromatograms of (A) metoprolol, (B) desmethyl metoprolol, (C) α-hydroxy metoprolol, (D) *N*-desisopropyl metoprolol, (E) blank and (F) IS at 10 ng/mL.

retention times of MET, HM, ODM and DIM were 1.3, 1.1, 1.2 and 1.05 min, respectively.

Bioanalytical method validations

The method was validated according to FDA guidelines for the validation of the bioanalytical method (US Food and Drug Administration, 2001; see Supporting Information).

Pharmacokinetic study and liver tissue distribution study

Rats were fasted for 12 h with free access to water prior to pharmacokinetic study. Rats were orally administered with MET in saline through gavage of 2 mg/kg dose. After oral administration of 2 mg/kg, MET is known to exhibit dose-independent pharmacokinetics, complete absorption and low bioavailability (Yoon *et al.*, 2011).The intestinal and hepatic first-pass extraction contributes to the low bioavailability of MET in rats (Yoon *et al.*, 2011). Blood samples were collected at 5, 10, 20, 30, 45, 60, 90, 120, 150 and 180 min, vortexed thoroughly and centrifuged at 5000 rpm for 20 min at 4 °C. Plasma was collected and stored at −20 °C until analysis. The plasma samples from six adult female Sprague–Dawley rats were analyzed for quantification of MET, HM, ODM and DIM with the validated method described above. The plasma concentration–time curve from 0 h to infinity ($AUC_{0-\infty}$) was calculated by noncompartmental analysis with Kinetica 2000 software (version 3.0).

In tissue distribution study, three rats (200–250 g) were orally administered MET (2 mg/kg). Rats were then sacrificed at 0.50 h after dosing. Livers were removed, washed with normal saline, blotted dry with filter paper and then accurately weighed. The tissues were homogenized in saline solution (~100 mg/mL) and the homogenates were stored at − 20 °C until analysis.

Determination of protein binding of metoprolol and its metabolites and log*P* calculation

The standard stock solutions of MET, HM, ODM, DIM, warfarin and atenolol were prepared separately in methanol at a concentration of 10 mM. Working stock solutions of 10 μM each were prepared separately in rat plasma. An aliquot of 300 μL of plasma containing MET, HM, ODM and DIM was added to the red chambers of RED device insert, while 500 μL of phosphate buffer saline (PBS; pH 7.4) was added to the other chamber. The device was covered with immunoware sealing tape and incubated at 37 °C with shaking at 550 rpm for 5 h. The highly bound warfarin and lower bound atenolol to protein were compared with MET, HM, ODM and DIM to calculate percentage unbound to albumin protein. The percent of plasma unbound fraction was calculated by the following equation:

$$\%\,\text{Unbound} = 100 \times \text{FC}/\text{TC}$$

where FC is the free compound concentration as determined by the calculated concentration on the buffer side of the membrane and TC is the total compound concentration as determined by the calculated concentration on the plasma side of the membrane.

Log*P* values of MET, HM, ODM and DIM were generated using Molinspiration Cheminformatics web services (www.Molinspiration.com/services/logp.html).

Inhibition experiments in human liver microsomes to determine IC_{50} values

The incubation was performed in duplicate. Inhibition experiments were performed to determine IC_{50} value of quinidine for CYP2D6-catalyzed biotransformation of dextromethorphan to dextrorphan and ketoconazole for CYP3A4-catalyzed midazolam to 1-hydroxy midazolam. Similarly inhibitions experiments were performed for MET, HM, ODM and DIM for CYP2D6 and CYP3A4. Standard inhibitory concentration of inhibitors quinidine and ketoconazole was 0.01–3 μM, whereas that for MET, HM, ODM and DIM was 0.01–9.00 μM. HLMs (0.1 mg/mL) and substrates (final 5 μM dextromethorphan and 2 μM midazolam based on their K_m values) were pre-incubated for 10 min at 37 °C before reaction were initiated by adding NADPH (1 mM, final concentration). The reaction was terminated by adding 200 μL cold ACN containing 10 ng/mL atenolol as IS. The samples were vortexed, centrifuged at 4000 rpm for 20 min and the supernatant from each sample was injected into UPLC/ESI/HRMS for analysis. In brief, Hypersil gold C_{18} column (50 × 2.1 mm i.d.; particle size 3 μm), C_{18} HQ105 (10 × 2.1 mm) guard column and mobile phase consisting of a mixture of 0.1% formic acid–acetonitrile (30:70) in an isocratic elution mode were used to measure 1-OH midazolam and dextrorphan (Borkar *et al.*, 2014). The metabolites were estimated in presence of their selective standard inhibitor. The HRMS EICs of 1-OH midazolam and dextrorphan showed their elution times at 1.4 and 1.3 min, respectively. The amount of dextrorphan and 1-hydroxy midazolam in each sample (relative to negative control samples) was plotted vs concentration of the inhibitor present. A sigmoid-shaped curve was fitted to the data and IC_{50}s calculated using GrapPad Prism software.

In vitro CYP interaction screening data was generated for CYP2D6 and CYP3A4 with an arbitrary fixed concentration (3 μM) of selective CYP chemical inhibitors (Feng *et al.*, 2002). This approach decreased the number of samples necessary to calculate the IC50 value for DDI, amount of the drug, liver microsomes, recombinant CYPs, probe substrate, reagents and analytical instrumentation time needed to determine the IC_{50} in early drug discovery. A series of incubations were also performed in the absence of specific CYP450 inhibitors, MET, HM, ODM and DIM. The percentage activities of the main metabolites of the substrates were measured in the presence of specific standard inhibitors and MET metabolites. The percentage activity of metabolites, free of standard inhibitors, MET, HM, ODM and DIM, was defined as 100%.

Results

Identification and characterization of *in vitro* and *in vivo* metabolites MET

To elucidate the structures of the unknown metabolites, we studied the fragmentation of the $[M+H]^+$ ions of MET (Borkar *et al.*, 2012) and its metabolites using LC/ESI/MS/MS experiments in combination with accurate mass measurements. Major metabolites such as HM and ODM were compared with the retention time of the commercial reference standards. The other metabolites were metoprolol acid (1.2 min), DIM (1.6 min) and *N*-dealkyl metoprolol acid (1.63 min). The product ions of the protonated metoprolol acid and *N*-desisopropylation of metoprolol are compared with the product ions of protonated MET to assign likely structures for the observed metabolites (Scheme S2, see the Supporting Information) The elemental composition of *N*-dealkyl metoprolol acid (*m/z* 241.10705 ($C_{12}H_{16}O_5$)) formed by oxidative deamination was confirmed by accurate mass measurements having an error of 1.92 ppm. Owing to the low abundance of *m/z* 241, *N*-dealkyl metoprolol acid, it was not further selected for MS/MS fragmentation. HM, ODM, *N*-dealkyl metoprolol acid and metoprolol acid metabolites were formed in RLM, HLM, rat plasma and urine samples. Heart and intestinal microsomes showed the formation of only HM and ODM metabolites, whereas DIM was observed in RLM, HLM, rat plasma and urine samples. Treatment of plasma samples with β-glucuronidase and sulfatase does not change significantly MET, HM and ODM plasma concentrations. Similarly, *in vitro* glucuronidation/sulfation assay of MET revealed that MET is not metabolized via conjugating reaction in rats.

ESI/MS/MS protonated MET ($[M+H]^+$ *m/z* 268). The ESI/MS/MS spectrum of $[M+H]^+$ ion of 268 shows product ions at *m/z* 250 (loss of H_2O), *m/z* 226 (loss of -CH_3-CH = CH_2), *m/z* 218 (loss of -CH_3OH from *m/z* 250), *m/z* 191 (loss of -$C_3H_7NH_2$ from *m/z* 250), *m/z* 176 (loss of -CH_3-CH = CH_2 from *m/z* 218), *m/z* 159 (loss of -CH_3OH from *m/z* 191), *m/z* 133 (loss of $CH_2 = CH_2$ from *m/z* 159), *m/z* 121 (-$C_3H_3NH_2$ from *m/z* 176), *m/z* 116 [loss of 4-(2-methoxyethyl)phenol], *m/z* 98 (loss of H_2O from *m/z* 116), *m/z* 74 (loss of -C_3H_6 from *m/z* 116), *m/z* 72 (loss of -C_3H_8 from *m/z* 116) and *m/z* 56 (loss of H_2O from *m/z* 74 (Fig. 3; Scheme 1; Borkar *et al.*, 2012). The elemental compositions of all the fragment ions were confirmed by accurate mass measurements (Table 1).

ESI/MS/MS of protonated *N*-desisopropyl metoprolol metabolite ($[M+H]^+$ *m/z* 226). The metabolite DIM at *m/z* 226.1441 ($[M+H]^+$) with an elemental composition of $C_{12}H_{20}NO_3$, was eluted at 1.6 min (Fig. 4a). The decrease of 42 Da in molecular weight (NH-CH-CH_3-CH_3 → NH_2) as compared with MET indicates that the metabolite is *N*-desisopropylated (Fig. 4b; Scheme 2). The details of protonated DIM metabolite fragmentation are given in the Supporting Information. The elemental compositions of DIM and its fragment ions were confirmed by the accurate mass measurements (Table 2).

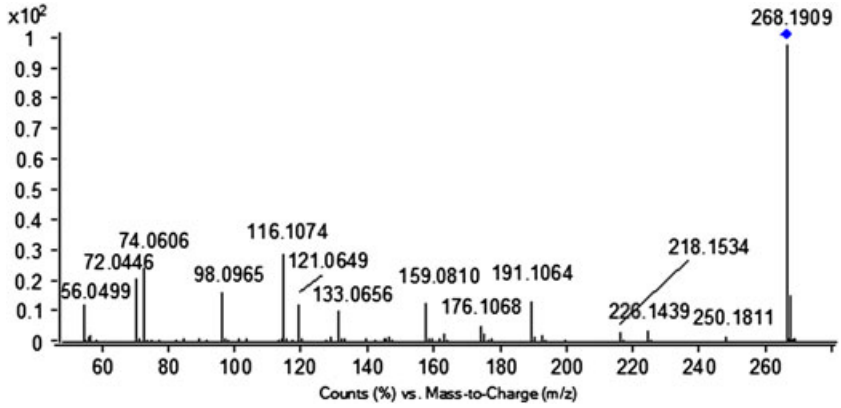

Figure 3. Positive ion LC/ESI/MS/MS spectrum of protonated metoprolol (*m/z* 268.1909).

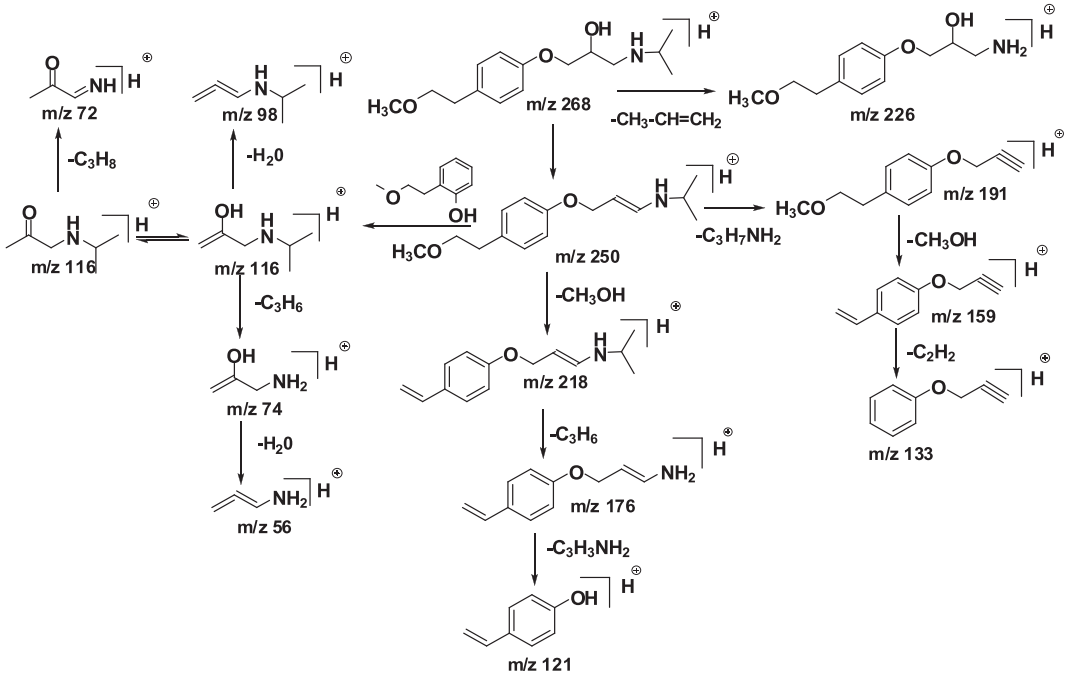

Scheme 1. Proposed fragmentation mechanism for protonated metoprolol (*m/z* 268).

ESI/MS/MS of protonated metoprolol acid metabolite ($[M + H]^+$ *m/z* 268). The metabolite metoprolol acid at *m/z* 268.1546 ($[M + H]^+$) with an elemental composition of $C_{14}H_{22}NO_4$, was eluted at 1.24 min (Fig. 5a). The molecular weights of metoprolol acid and metoprolol are the same but differ in elemental compositions (Fig. 5b; Scheme 3). The details of protonated metoprolol acid metabolite fragmentation are given in the Supporting Information. The elemental compositions of metoprolol acid and its fragment ions were confirmed by the accurate mass measurements (Table 1).

Determination of plasma protein binding of MET, HM, ODM and DIM using RED device

Drug bound to plasma protein such as albumin and α-1 acid glycoprotein limits the availability of free drug concentration in plasma. The ratio of free and plasma protein-bound drugs will have an impact on safety margins of the compounds (Wan and Bergstrom, 2007). A highly protein-bound standard drug warfarin and low bound drug atenolol, at a pharmacological drug concentration of 10 μM showed the percentage bound (±SD; CV, %) to be 99.76% (±0.04; 0.15) and 4.22% (±0.38; 9.06), respectively. The determined values of the percentage bound (±SD; CV, %) of MET, HM, ODM and DIM were 13.41 (±0.29; 2.18), 4.76 (±0.64; 13.47), 6.88 (±0.88; 12.83) and 11.43 (±0.32; 7.18) respectively.

Quantification of total (bound and unbound) and unbound MET, HM and ODM

The validated method was utilized to measure the concentrations in plasma of total (bound and unbound) MET, HM, ODM and DIM to protein and the unbound drug after administration of a single oral dose of 2 mg/kg. At 2 mg/kg, MET exhibited dose-independent pharmacokinetics, complete absorption and low bioavailability (Yoon *et al.*, 2011). The major pharmacokinetic parameters were calculated by a noncompartmental analysis with Kinetica 2000 software (version 3.0). As shown in Fig. 6 the maximum plasma concentration (C_{max}) of MET, time at which the concentration reached the maximum (T_{max}) and the terminal half-life ($t_{1/2}$) were 102.17 ± 3.11 ng/

Table 1. Elemental compositions for daughter ion of metoprolol *m/z* 268

Drug	Proposed formula	Observed mass (Da)	Theoretical mass (Da)	Error (ppm)
Metoprolol	$C_{15}H_{26}NO_3$	268.1909	268.1912	1.11
	$C_{15}H_{24}NO_2$	250.1811	250.1807	−1.59
	$C_{12}H_{20}NO_3$	226.1439	226.1443	1.76
	$C_{14}H_{20}NO$	218.1534	218.1544	4.58
	$C_{12}H_{15}O_2$	191.1064	191.1072	4.18
	$C_{11}H_{14}NO$	176.1068	176.1075	3.97
	$C_{11}H_{11}O$	159.081	159.0809	−0.62
	C_9H_9O	133.0656	133.0653	−2.25
	C_8H_9O	121.0649	121.0653	3.30
	$C_6H_{14}NO$	116.1074	116.1075	0.86
	$C_6H_{12}N$	98.0965	98.0969	4.07
	C_3H_8NO	74.0606	74.0605	−1.35
	C_3H_6NO	72.0446	72.0447	−1.38
	C_3H_5O	57.0341	57.0340	−1.75
	C_3H_6N	56.0499	56.0500	1.78

mL, 0.3–0.5 h and 0.73 ± 0.07 h, respectively (Table 3). The plasma concentration–time curve from 0 h to the last measurable concentration (AUC_{0-t}) and area under plasma concentration–time curve from 0 h to infinity ($AUC_{0-\infty}$) for total MET were 74.99 ± 5.57 and 78.45 ± 6.66 ng h/mL, respectively. The values of C_{max} of HM, ODM and DIM were 35.03 ± 1.80, 18.53 ± 1.68 and 7.96 ± 0.94 ng/mL, respectively. The AUC_{0-t} and $AUC_{0-\infty}$ for HM were 43.92 ± 3.4 and 50.75 ± 3.18 ng h/mL, respectively while the AUC_{0-t} and $AUC_{0-\infty}$ for ODM were 19.58 ± 3.09 and 19.84 ± 3.00 ng h/mL, respectively. The AUC_{0-t} and $AUC_{0-\infty}$ for DIM were 10.66 ± 0.58 and 19.00 ± 1.25 ng h/mL, respectively. The total AUC_m/AUC_p ratios were ≥0.25 for HM and ODM (Table 4). On the other hand the unbound AUC_m/AUC_p ratios were ≥0.25 for HM and ODM. In addition, HM ODM and DIM AUCs were >10% of total drug related material as HM was 34%, ODM was 13% and DIM was 11% of the total quantified drug-related material in this study. The circulating metabolites, HM and ODM, were found to be have exposures of >25% that of MET when either the total or unbound ratio AUCs of metabolites to drug were considered, hence metabolites were evaluated for *in vitro* inhibitory potential and included *in vivo* risk assessment. However, other metabolites such as DIM only met the criteria of > 10% of total drug related material. As such it is unclear if testing of this quantitatively DIM metabolite would be considered necessary. Treatment of plasma samples with β-glucuronidase and sulfatase did not change the concentrations of MET, HM ODM and DIM. Similarly, *in vitro* glucuronidation/sulfation assay of MET revealed that MET is not metabolized via conjugating reaction in rats.

*Clog*P values of MET and its metabolites were calculated and the values are listed in Table 4. All metabolites were less lipophilic than MET. When the log*P* values were compared with the fraction of unbound plasma for MET and its metabolites, increased *Clog*P value of MET was associated with increased plasma protein binding and decreased fraction of unbound in plasma. Metabolites HM, ODM and DIM were less bound to plasma proteins and the fraction unbound in plasma increased.

Tissue distribution study of MET

The validated method was used to determine the concentration of the MET, HM, ODM and DIM in liver tissue after administration of a single oral dose. Hepatic metabolism is a primary route of elimination for the majority of the drug, hence liver was used. The concentrations of MET, HM, ODM and DIM in liver tissue at 0.50 h were 0.87 ± 0.12, 0.23 ± 0.01, 0.12 ± 0.03 and 0.15 ± 0.03 ng/mg, respectively (Fig. 7).

Molecular docking studies

The binding affinity between each MET metabolites to CYP2D6 and CYP3A4 was studied respectively owing to uncertainty for minor

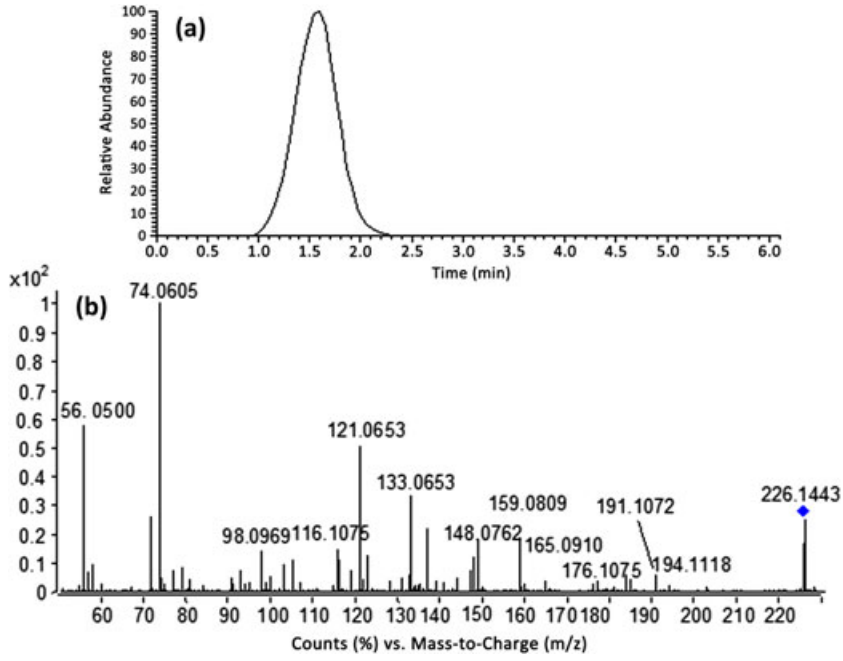

Figure 4. (a) Extracted ion chromatogram *N*-deisopropyl metoprolol metabolite [formed in rat liver microsomes (RLMs), human liver microsomes (HLMs), rat urine and feces] eluted at 1.6 min and (b) positive ion LC/ESI/MS/MS spectrum of protonated *N*-deisopropyl metoprolol metabolite (*m/z* 226.1443).

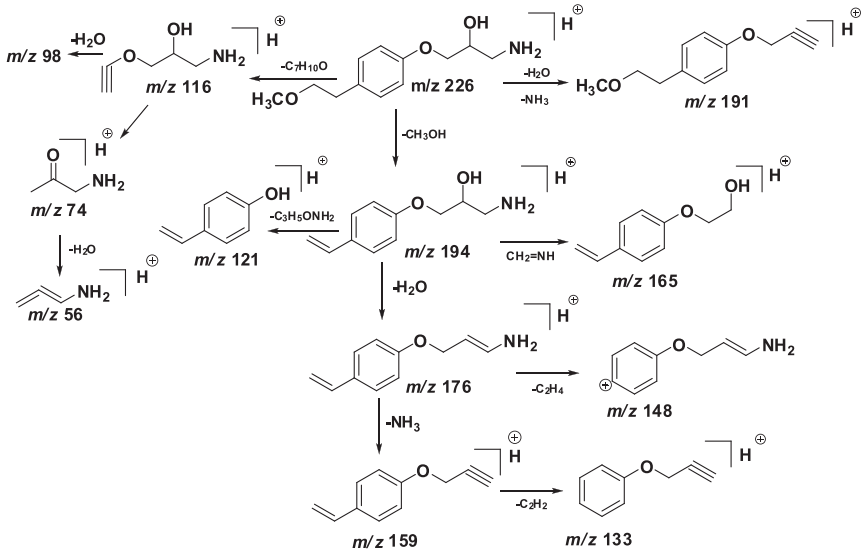

Scheme 2. Proposed fragmentation mechanism for protonated *N*-desisopropyl metoprolol metabolite (*m/z* 226).

Table 2. Elemental compositions for daughter ion of *N*-deisopropyl metoprolol and metoprolol acid

Metabolites	Proposed Formula	Observed mass (Da)	Theoretical mass (Da)	Error (ppm)
N-Deisopropyl metoprolol	$C_{12}H_{20}NO_3$	226.1443	226.1441	0.88
	$C_{11}H_{16}NO_2$	194.1181	194.118	0.51
	$C_{12}H_{15}O_2$	191.1072	191.1069	1.56
	$C_{11}H_{14}NO$	176.1075	176.1069	3.40
	$C_{10}H_{13}O_2$	165.091	165.0916	−3.63
	$C_{11}H_{12}O$	159.0809	159.081	−0.62
	$C_9H_{10}NO$	148.0762	148.0756	4.05
	C_9H_9O	133.0653	133.0657	−3.00
	C_8H_9O	121.0653	121.0648	4.13
	$C_5H_{10}NO_2$	116.1075	116.1078	−2.58
	$C_5H_{10}NO_2$	98.0969	98.0966	3.05
	C_3H_8NO	74.0605	74.0603	2.70
	C_3H_6N	56.0500	56.0501	−1.78
Metoprolol acid	$C_{14}H_{22}NO_4$	268.1548	268.1546	0.74
	$C_{14}H_{20}N0_3$	250.1443	250.1445	−0.79
	$C_{11}H_{11}O_3$	191.0708	191.0711	−1.57
	$C_{14}H_{18}NO$	216.1383	216.1377	2.77
	$C_{11}H_{16}NO_4$	226.1079	226.1081	−0.88
	$C_{11}H_{14}NO_3$	208.0973	208.0981	−3.84
	$C_{10}H_{16}NO_2$	182.1181	182.1179	1.09
	$C_8H_70_2$	135.0446	135.0443	2.22
	C_7H_7	91.0547	91.0544	3.29

metabolites of the quantified metabolites for DDI risk assessment. Minor metabolites such as metoprolol acid, DIM and *N*-dealkyl metoprolol acid were evaluated for the binding affinity on CYP2D6 and CYP3A4 in DDI risk assessment. Results of molecular docking of ligands to CYP2D6 showed that the docking score of *N*-dealkyl metoprolol acid (−5.4 kcal/mol) to the active cavity was comparable to that of quinidine (−5.4 kcal/mol), greater than that of metoprolol acid (−3.7 kcal/mol) and less than that of DIM (−6.7 kcal/mol) (Fig. 8F). The model probe substrate dextromethorphan and inhibitor quinidine bind to the same biding site in CYP2D6 to cause competitive inhibition for the catalytic site (McLaughlin *et al*., 2005). *N*-dealkyl metoprolol acid showed similar affinity to quinidine in binding to the catalytic site on CYP2D6. Metoprolol acid showed much lower affinity than quinidine and therefore are unlikely to compete for the binding site on CYP2D6 whereas DIM has more affinity. Results of the molecular docking of ligands to CYP3A4 showed that the logarithm of free binding energy of *N*-dealkyl metoprolol acid (−4.6 kcal/mol), DIM (−4.5 kcal/mol) and metoprolol acid (−4.9 kcal/mol) showed much lower affinity than ketoconazole (−6.4 kcal/mol) and therefore they are unlikely to compete for the binding site on CYP3A4 (Fig. 9F).

The atomic level ligand–protein interactions were observed for better understanding of *N*-dealkyl metoprolol acid, DIM and metoprolol acid (Fig. 8A–E). It has been reported that Phe120, Glu216, Asp301, Phe481 and Phe483 are key amino acid residues for substrate interaction within in the active site of CYP2D6 (McLaughlin *et al*., 2005; Unwalla *et al*., 2010). Alanine substitution of Phe120 had only a minor effect on the inhibition and binding activity, whereas alanine substitution of Glu216 and Asp301 played a significant role in binding to CYP2D6 active site in productive orientation. In the present study, the interactions of Phe120, Glu216 and Asp301 amino acid residues with ligands were investigated. Interactions of these amino acid residues with metoprolol acid, DIM and *N*-dealkyl metoprolol acid were investigated and the results showed that Phe120 and Asp301 are critical for the binding of the DIM to the active cavity, but not to Glu216. The benzene ring of DIM provided a π–π interaction with Phe120, which may offer an optional conformation, and contributed to higher binding energy of −6.7 kcal/mol. *N*-Dealkyl metoprolol acid and metoprolol acid did not show any interaction with Phe120 or any other amino acids residues such as Glu216 andAsp301. From molecular docking of *N*-dealkyl metoprolol acid in CYP3A4, a π–π interaction of benzene ring and hydrogen bonding between hydroxy group of ligand with Arg212 was observed. The binding cavity of CYP3A4 was lined by residue Glu374 and Arg212 and formed hydrogen bonding with free hydroxy and methoxy oxygen of DIM, respectively. Whereas Arg212 formed hydrogen bonding with the carboxyl group of metoprolol acid and Phe215, Phe57 formed π–π stacking (Fig. 9A–E).

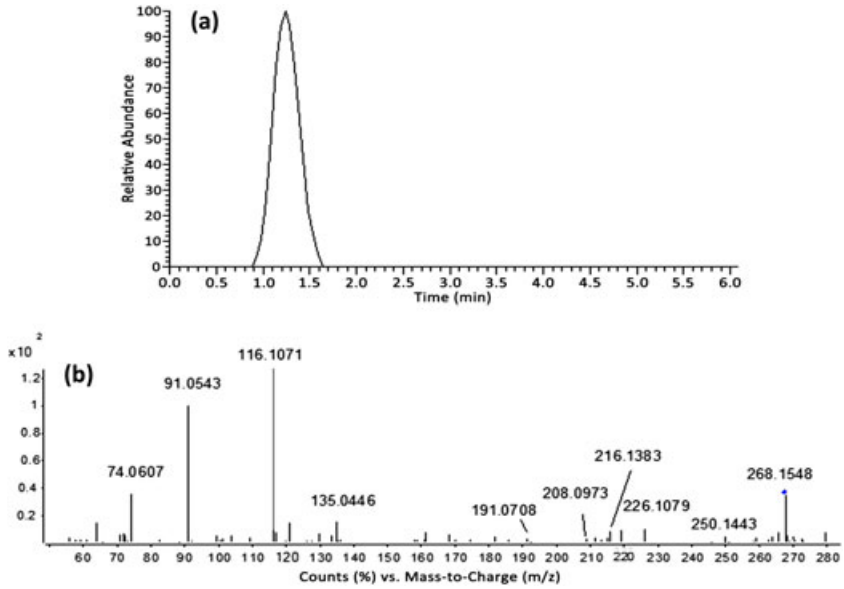

Figure 5. (a) Extracted ion chromatogram of metoprolol acid (formed in RLMs, HLMs, rat urine and feces) metabolite eluted at 1.24 min and (b) positive ion ESI/MS/MS spectrum of protonated metoprolol acid metabolite (*m/z* 268.1546).

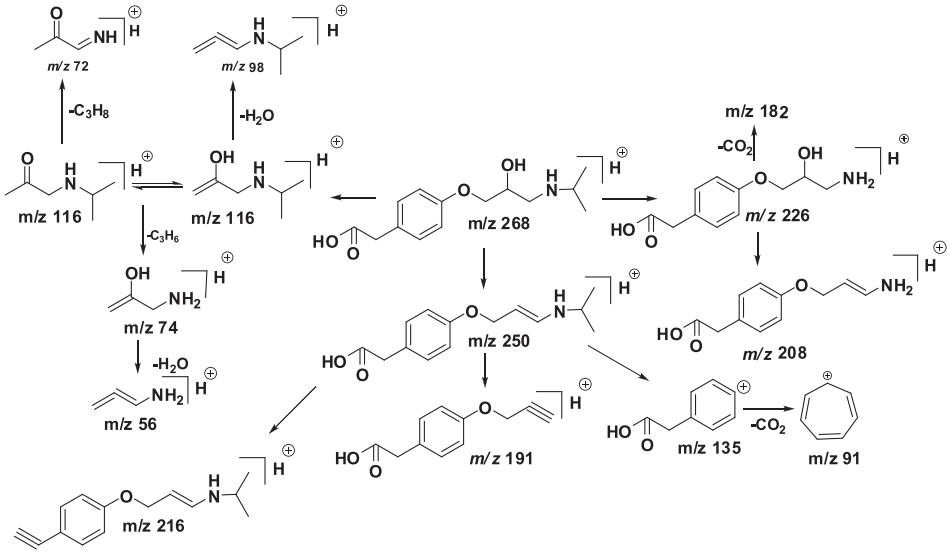

Scheme 3. Proposed fragmentation mechanism for protonated metoprolol acid metabolite (*m/z* 268).

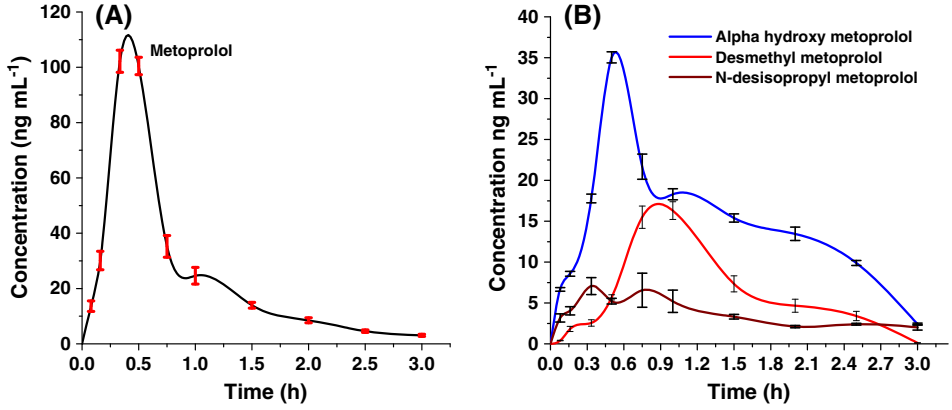

Figure 6. Mean plasma concentration time profile of (A) metoprolol and (B) α-hydroxy metoprolol desmethyl metoprolol and *N*-desisopropyl metoprolol in plasma. All values are mean ± standard error mean (SEM).

Table 3. Pharmacokinetic parameters of metoprolol and its metabolites after oral (p.o.) administration of metoprolol at dose 2 mg/kg to rats ($n = 6$)

Pharmacokinetic parameter	Metoprolol	α-Hydroxymetoprolol	Desmethyl metoprolol	*N*-Desisopropyl metoprolol
C_{max} (ng/mL)	102.18 ± 3.12	35.04 ± 1.81	18.53 ± 1.69	7.96 ± 0.94
T_{max} (h)	0.33 (0.33–0.5)	0.5	0.75 (0.75–1)	0.33 (0.33–0.5)
$t_{1/2}$ (h)	0.73 ± 0.08	1.95 ± 0.26	1.66 ± 0.22	2.15 ± 0.14
Elimination rate constant	0.93 ± 0.14	0.36 ± 0.04	0.43 ± 0.06	0.28 ± 0.02
AUC_{0-3} (ng h/mL)	74.99 ± 5.57	43.92 ± 3.40	19.58 ± 3.09	10.66 ± 0.58
$AUC_{0-\infty}$ (ng h/mL)	78.46 ± 6.67	50.75 ± 3.18	19.85 ± 3.00	19.01 ± 1.25

Values are expressed as means ± standard deviation except median (ranges) for T_{max}.
C_{max}, Maximum plasma concentration; T_{max}, time at which the concentration reached the maximum; $t_{1/2}$, terminal half-life; AUC, area under plasma concentration–time curve.

Table 4. Log*P*, fraction unbound plasma and ratio of AUC_m/AUC_p values of metoprolol and its metabolites

Inhibitors	*Clog*P	Fraction unbound Plasma	AUC_m/AUC_p		AUC_m/AUC_t[a]
			Total $AUC_{0-\infty}$	Unbound$AUC_{0-\infty}$	Total $AUC_{0-\infty}$
MET	1.97	0.86 ± 0.02	—	—	—
HM	0.98	0.95 ± 0.06	0.65	0.71	≤0.34
DMT	1.35	0.93 ± 0.08	0.26	0.27	≤0.13
DIM	0.32	0.89 ± 0.03	0.24	0.24	≤0.11

[a]In the absence of a mass balance study, total drug-related material was estimated as a fraction of all quantified compounds.

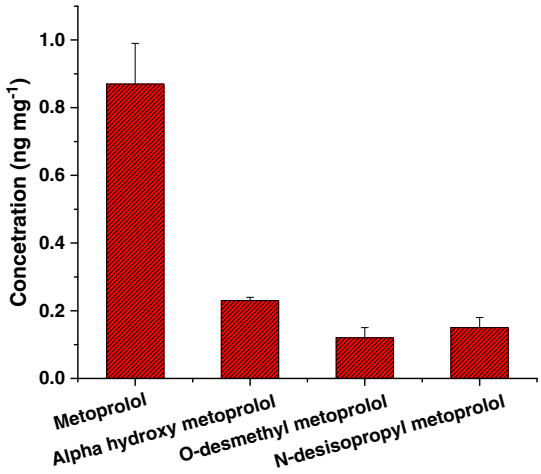

Figure 7. Concentrations metoprolol and its metabolites in liver tissue at 0.50 h after single oral administration in rats. All values are mean ± SEM.

Molecular docking study revealed DIM may act as a competitive inhibitor in binding to the catalytic site of CYP2D6; hence it was further selected for synthesis, pharmacokinetic study and to evaluate the *in vitro* inhibition potential for CYP2D6.

In vitro inhibition of CYP2D6 and CYP3A4 by metoprolol and its metabolites

Inhibition potential of MET, HM, ODM and DIM was evaluated in pooled HLMs for CYP2D6 and CYP3A4 enzymes. Dextromethorphan (CYP2D6 substrate) and midazolam (CYP3A4 substrate) and were treated with HLMs in presence of their specific inhibitors quinidine and ketoconazole, respectively, and MET, HM, ODM and DIM. A sigmoid-shaped curve was fitted to the *in vitro* CYP inhibition data that was generated for CYP2D6 and CYP3A4. IC_{50} values were calculated using GrapPad Prism software. Inhibition (%) curves for ketoconazole, quinidine and DIM obtained from *in vitro* CYP inhibition experiments are shown in Fig. 10(A–C) and the best-fit log IC_{50} value determined from the data is displayed on each graph. The percentage activities of 1-OH midazolam and dextrorphan were 5.28 ± 1.21 and 3.44 ± 1.56%, respectively, in the presence of their specific inhibitors ketoconazole and quinidine at 3 μM. The effects of the HM, ODM and DIM on the percentage activity of 1-OH midazolam and dextrorphan are shown in Fig. 10(D and E). MET, HM and ODM were not found to inhibit CYP3A4-catalyzed midazolam metabolism (percentage activity of 1-OH midazolam, 94.43 ± 6.63 for HM, 97.80 ± 5.68 for ODM and 93.79 ± 3.12 for MET) and CYP2D6 catalyzed dextromethorphan metabolism (percentage activity of 1-dextrorphan 103.24 ± 5.84 for ODM, 98.03 ± 4.67 for HM and 89.45 ± 2.66 for MET). In addition the minor metabolite DIM was found inhibit CYP2D6 catalyzed dextromethorphan metabolism (percentage activity of 1-dextrorphan 23.34 ± 3.54).

Discussion and conclusion

The FDA and EMA have recommended the testing of CYP450 inhibition potential of drug metabolites. This may not include the inhibition potential of the drug during *in vivo* DDI. Few studies have reported the importance of the metabolites in *in vivo* DDI (Templeton *et al.*, 2008; Yeung *et al.*, 2011; Yeo *et al.*, 2010; Zhang *et al.*, 2009). However, the correlation of the circulating level of metabolites and their importance in DDIs are unclear. *N*-Desalkyl-

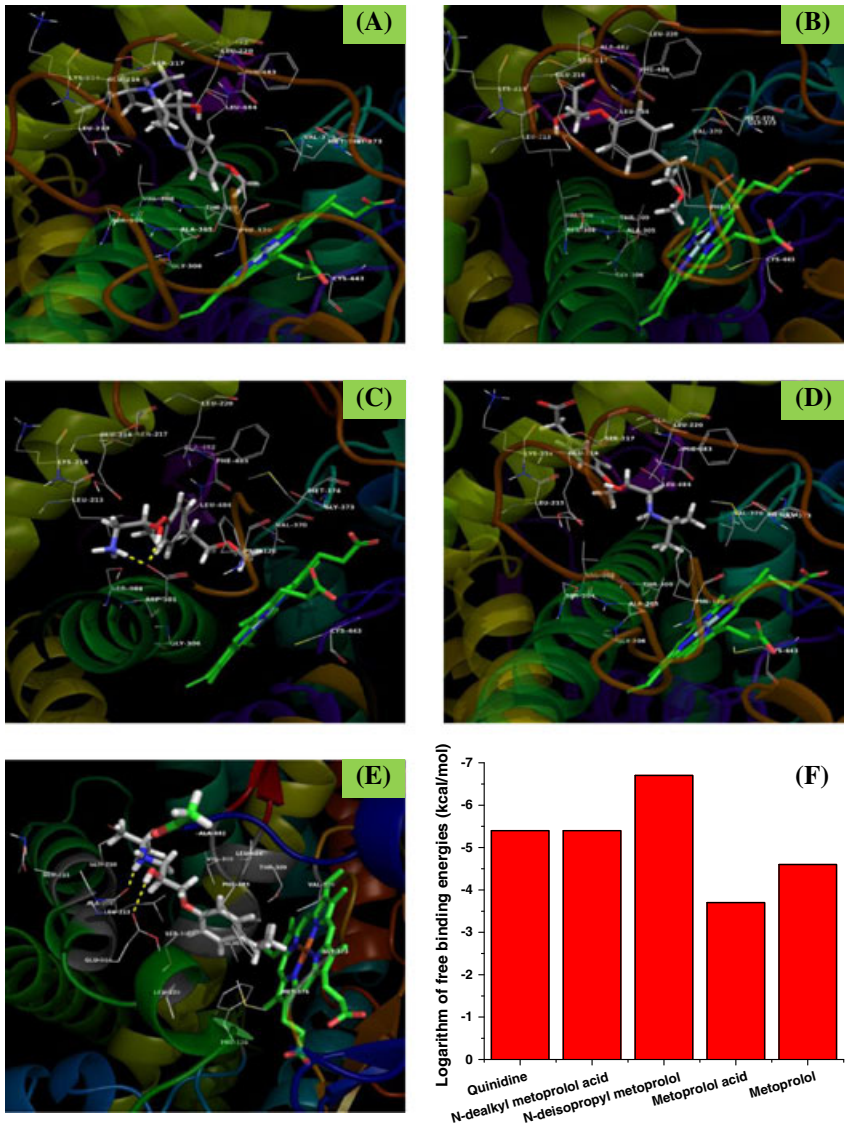

Figure 8. The binding pose of ligands showing the most energetically favorable binding modes of quinidine (A), *N*-dealkyl metoprolol acid (B), *N*-deisopropyl metoprolol (C), metoprolol acid (D) and metoprolol (E) at the drug-binding cavity of CYP2D6 (PDB code 2F9Q) and comparison of free binding energies (kcal/mol) of docked ligands (F).

itraconazole and hydroxy-itraconazole, minor and major metabolites of a CYP3A4 inhibitor itraconazole, respectively, have been predicted to have similar importance in *in vivo* DDI (Templeton *et al*., 2008). Similarly to the CYP2D6 inhibitor bupropion, metabolites have been reported (Yeung *et al*., 2011). Yu and Tweedie (2013) recommended the consideration of log*P* value of metabolites for testing the inhibition potential of metabolites. The log*P* value of metabolites will address the issue of the circulating level of metabolites and its importance in DDIs. The aim of this study was to determine, considering MET as an example, the contribution of total circulating or unbound metabolites that could be used to guide in *in vitro* DDIs of metabolite testing regardless of their log*P* value and abundance.

Initially, circulating metabolites of MET were identified and characterized. The metabolites formed were HM, ODM, DIM, metoprolol acid and *N*-dealkyl metoprolol acid. MS/MS fragmentations of metabolites were not reported earlier. Intestinal and heart microsomes were used to identify the involvement of extra hepatic tissue in the metabolism of MET. Intestinal and cardiac CYPs inhibition risk assessment by circulating metabolites is unclear; hence DDI and DHI do not consider the inhibition of extra hepatic CYP450 enzymes. MET undergoes metabolism in extra-hepatic tissue such as intestinal and cardiac. Both intestinal and cardiac tissues are involved in the formation of HM and ODM.

DDI risk assessment for minor metabolite of the quantified metabolites is unclear; hence a molecular docking study was performed for minor metabolites such as metoprolol acid, DIM and *N*-dealkyl metoprolol acid for the binding affinity on CYP2D6 and CYP3A4 in DDI risk assessment. *N*-Dealkyl metoprolol acid showed similar affinity to quinidine, a model for CYP2D6 inhibitor, in binding to the catalytic site on CYP2D6, but it did not interact with either Asp301 or Glu216, which generally interacted with typical CYP2D6 substrates (Kotsuma *et al*., 2009). Phe120, a key amino acid residue, was very important in the terms of selection and region specification of substrates binding to CYP2D6. Amino acid residues Phe120, Glu216 and Asp301 are important in determining the productive or nonproductive mode of binding of quinidine to CYP2D6 (McLaughlin *et al*., 2005). The benzene ring of DIM provided a π–π

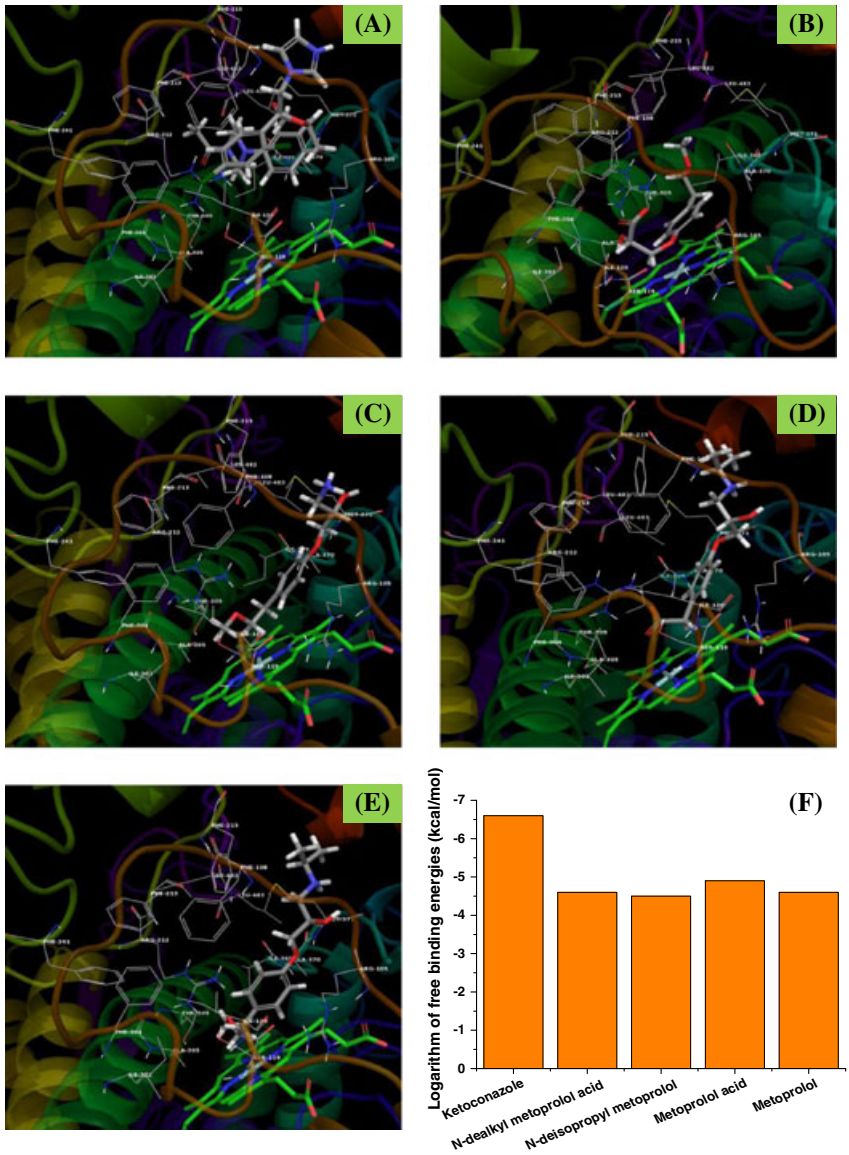

Figure 9. The binding pose of ligands showing the most energetically favorable binding modes of ketoconazole (A), *N*-dealkyl metoprolol acid (B), *N*-deisopropyl metoprolol (C), metoprolol acid (D) and metoprolol (E) at the drug-binding cavity of CYP3A4 (PDB code 1TQN) and comparison of free binding energies (kcal/mol) of docked ligands (F).

interaction with Phe120, contributing higher binding energy of −6.7 kcal/mol and may act as a competitive inhibitor in binding to the catalytic site of CYP2D6. The binding energy of DIM to Phe120 was greater than that of quinidine, indicating that it has greater affinity in binding to the catalytic site on CYP2D6. Moreover, *N*-dealkyl metoprolol acid did not interact with the key residues Glu216 and Asp301 and it may not be the substrate for CYP2D6.

In several studies a bioanalytical method has been developed and validated in biological samples for the determination of MET and its metabolites, but lacking quantification of HM and ODM. Recently Rao *et al.* (2015) developed an LC-MS/MS method for the determination of MET, HM and ODM in rat plasma after administration of 40 mg/kg of MET to rats for DHI. At 40 mg/kg dose, MET will not show first-pass extraction in rat, which may lead to potential bias in the pharmacokinetic analysis of MET, HM and ODM in DDI and DHI issues. However, Yoon *et al.* (2011) observed dose-independent pharmacokinetics, complete absorption at 1 and 2 mg/kg doses of MET and dose-dependent pharmacokinetics at a dose of 5 mg/kg, most probably owing to the saturation of first-pass extraction of MET. Considerable hepatic and intestinal first-pass extraction of MET in rats has been observed. Hence in the current study it is anticipated that a 2 mg/kg dose of MET would not saturate the hepatic and intestinal first-pass extraction and pharmacokinetic analysis of drug and its metabolites would remain unbiased for DDI and DHI. Therefore a new bioanalytical method has been developed and validated for the determination of MET, HM, ODM and DIM in rat plasma and liver tissue and applied to the pharmacokinetics of the drug and its metabolites. The drug and its metabolites have been quantified after administration of 2 mg/kg of MET to rats. Quantified metabolites were evaluated for *in vitro* CYP450 inhibition if they met the criteria of $AUC_m/AUC_p \geq 0.25$ for circulating metabolites described by the FDA and EMA. However, HM and ODM meets the criteria of >25% of the parent using unbound concentrations and AUC are >10% of total drug-related material. However, DIM only meets

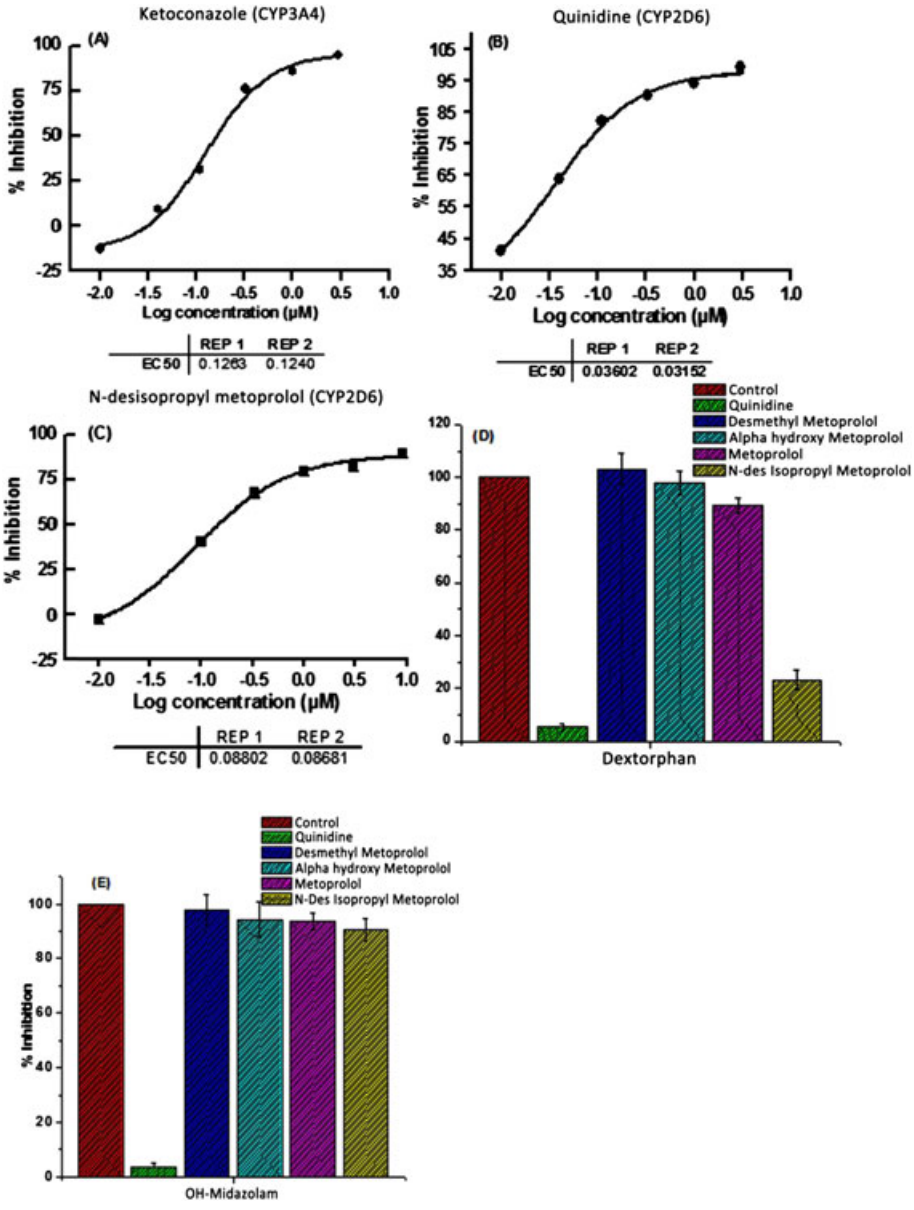

Figure 10. NADPH-dependent IC_{50} of standard inhibitors: (A) ketoconazole (0.01–3 μM) for CYP3A4 catalyzed midazolam to 1-hydroxy midazolam; (B) quinidine (0.01–3 μM) for CYP2D6 dextromethorphan to dextrorphan in HLMs; and (C) *N*-desisopropyl metoprolol (0.01–9 μM) for CYP2D6. (D) CYP2D6 and CYP3A4 inhibition potential of desmethyl metoprolol, α-hydroxy metoprolol, metoprolol and *N*-desisopropyl metoprolol with respect to specific inhibitor: quinidine for dextromethorphan to dextrorphan by CYP2D6 and ketoconazole for midazolam to 1-hydroxy midazolam by CYP3A4. The percentage activity of metabolite dextrorphan was defined as 100% when HLMs were free of inhibitors, α-hydroxy metoprolol (3 μM), desmethyl metoprolol (3 μM) and metoprolol (3 μM). All values are means ± SEM.

the criteria of >10% of the total drug-related material and <25% of the parent using unbound concentrations. The IC_{50} value of DIM was 0.08 μM, which is approximately equal to the $AUC_{0-\infty}$ concentration of DIM. MET and its metabolites were found to be present in liver tissue. Hepatic clearance may impact the oral bioavailability and thereby influence the drug dose and frequency of administration. It is unclear regarding the role of minor metabolites in DDI risk assessment. If CYP inhibition testing is solely based on metabolite exposure, DIM metabolite would probably to be not considered. Furthermore the EMA guideline suggests that the testing of quantitatively minor metabolite is not required. However DIM was the only metabolite of MET that is expected to contribute to *in vivo* DDIs in CYP2D6 and evaluation of other metabolites HM and ODM for CYP2D6 inhibition could be considered redundant. Hence it is necessary to reconsider the selection criteria of metabolites for risk assessment of DDI and ensure that minor metabolites which are important for DDI or DHI are tested irrespective of their abundance. Testing of the metabolites is also based on the lipophilicity of metabolites. Metabolites should circulate at concentrations >100% of the parent drug if the former is less lipophilic and may be considered for reversible inhibition. In the present study, all of the quantified metabolites were estimated to be less lipophilic than MET.

Identification of CYP inhibition potential of MET and its metabolites is the key element for DDI and DDH interactions. However the literature revealed that MET is not characterized for CYP450 enzyme inhibition studies. *In vitro* CYP2D6 and CYP3A4 inhibition studies of MET, HM, ODM and DIM revealed that both HM and

ODM were not inhibitors of CYP3A4-catalyzed midazolam metabolism and CYP2D6-catalyzed dextromethorphan metabolism in HLMs whereas DIM inhibited the CYP2D6 catalyzed reaction.

In conclusion, the results of this study show that, although the ratio of AUC of metabolites to parent drug is >25%, MET, HM and ODM did not inhibit the CYP2D6 and CYP3A4 enzymes in HLMs and there will be no role in DDI or DHI from the drug and its metabolites. However, DIM only meets the criteria of >10% of the total drug-related material and AUCm having <25% of the parent using unbound concentrations but inhibiting the CYP2D6 enzyme in HLMs. Docking experiments showed that DIM may act as a competitive inhibitor in binding to the catalytic site of CYP2D6. Minor metabolites may also contribute to *in vivo* DDIs or DHIs and their importance may not be related to their relative abundance in plasma. Hence it is important that the metabolites that are important in DDIs should be tested irrespective of their log*P* values and abundance in circulation. Extra-hepatic CYP enzymes are involved in the metabolism of MET. Extra-hepatic CYP450 inhibition by systemically formed metabolites should also be assessed in DDI or DHI risk analysis as they are also involved in the generation of metabolites.

Acknowledgments

The authors thank Dr S Chandrasekhar, Director, IICT, Hyderabad and Dr Ahmed Kamal, Project Director, National Institute of Pharmaceutical Education and Research, Hyderabad for facilities and their cooperation. Financial support was provided by the Ramalingaswami Fellowship fund (S.K.B.) from the Department of Biotechnology, CMET (CSC0110) and AARF (CSC0406) projects. R. M.B and M.M.B are thankful to CSIR, New Delhi, for awarding Senior Research Fellowship and Junior Research Fellowship, respectively. A.D, P.P and P.K are thankful to the Ministry of Pharmaceuticals, New Delhi, for providing Research Fellowships.

Authors' contributions

R.M.B., S.K.B. and R.S. conceived and designed the experiments. R. M.B., M.M.B., A.D. and P.K. performed the experiments. R.M.B., S.K.B. and R.S. analyzed the data. P.N. and A.S. performed the *in silico* study. V.G.R. and A.K. synthesized the compound. R.S. and S.K.B. contributed reagents/materials/analysis tools. R.M.B., S.K.B. and R. S. wrote the paper.

Conflicts of interests

The author declares no conflict of interest.

References

Barakat MM, El-Kadi AO and du Souich P. L-NAME prevents *in vivo* the inactivation but not the down-regulation of hepatic cytochrome P450 caused by an acute inflammatory reaction. *Life Science* 2001; **69**: 1559–1571.

Boralli VB, Coelho EB and Lanchote VL. Influence of quinidine, cimetidine, and ketoconazole on the enantioselective pharmacokinetics and metabolism of metoprolol in rats. *Chirality* 2009; **21**: 886–893.

Borkar RM, Raju B, Srinivas R, Patel P and Shetty SK. Identification and characterization of stressed degradation products of metoprolol using LC/Q-TOF-ESI-MS/MS and MS(*n*) experiments. *Biomedical Chromatography* 2012; **6**: 720–736.

Borkar RM, Bhandi MM, Dubey AP, Nandekar PP, Sangamwar AT, Banerjee SK and Srinivas R. Plasma protein binding, pharmacokinetics, tissue distribution and CYP450 biotransformation studies of fidarestat by ultra-high performance liquid chromatography–high resolution mass spectrometry. *Journal of Pharmaceutical and Biomedical Analysis* 2014; **102C**: 389–399.

Cerqueira PM, Coelho EB, Geleilete TJ, Goldman GH and Lanchote VL. Influence of chronic renal failure on stereo selective metoprolol metabolism in hypertensive patients. *Journal of Clinical Pharmacology* 2005; **45**: 1422–1433.

Chavez ML, Jordan MA and Chavez PI. Evidence based drug–herbal interactions. *Life Sciences* 2006; **78**: 2146–2157.

Cotreau MM, von Moltke LL, Beinfeld MC and Greenblatt DJ. Methodologies to study the induction of rat hepatic and intestinal cytochrome P450 3A at the mRNA, protein, and catalytic activity level. *Journal of Pharmacological and Toxicological Methods* 2000; **43**: 41–54.

Dunning T. Complementary therapies and diabetes. *Complementary Therapies in Nursing Midwifery* 2003; **9**: 74–80.

Edwards IR and Aronson JK. Adverse drug reactions: definitions, diagnosis, and management. *Lancet* 2000; **356**: 1255–1259.

European Medicines Agency. Guideline on the Investigation of Drug Interactions, 2012. Available from: http://www.ema.europa.eu/docs/en_GB/document_library/Scientific_guideline/2012/07/WC500129606.pdf (accessed 15 August 2014).

Feng G, Johnson DL, Ekins S, Janiszewski J, Kelly KG, Meyer RD and West M. Optimizing higher throughput methods to assess drug–drug interactions for CYP1A2, CYP2C9, CYP2C19, CYP2D6, rCYP2D6, and CYP3A4 in vitro using a single point IC(50). *Journal of Biomolecular Screening* 2002; **7**: 373–382.

Friesner RA, Banks JL, Murphy RB, Halgren TA, Klicic JJ, Mainz DT, Repasky MP, Knoll EH, Shelley M, Perry JK, Shaw DE, Francis P and Shenkin PS. Glide: a new approach for rapid, accurate docking and scoring. 1. Method and assessment of docking accuracy. *Journal of Medicinal Chemistry* 2004; **47**: 1739–1749.

Kaminski GA, Friesner RA, Tirado-Rives J and Jorgensen WL. Evaluation and reparametrization of the OPLS-AA force field for proteins via comparison with accurate quantum chemical calculations on peptides. *Journal of Physical Chemistry B* 2001; **105**: 6474–6487.

Kendall MJ, John VA, Quarterman CP and Welling PG. A single and multiple dose pharmacokinetic and pharmacodynamic comparison of conventional and slow-release metoprolol. *European Journal of Clinical Pharmacology* 1980; **17**: 87–92.

Kotsuma M, Hanzawa H, Iwata Y, Takahashi K and Tokui T. Novel binding mode of the acidic CYP2D6 substrates pactimibe and its metabolite R-125528. *Drug Metabolism and Disposition* 2009; **36**: 1938–1943.

Lasser KE, Allen PD, Woolhandler SJ, Himmelstein DU, Wolfe SM and Bor DH. Timing of new black box warnings and withdrawals for prescription medications. *Journal of the American Medical Association* 2002; **287**: 2215–2220.

McLaughlin LA, Paine MJ, Kemp CA, Maréchal JD, Flanagan JU, Ward CJ, Sutcliffe MJ, Roberts GC and Wolf CR. Why is quinidine an inhibitor of cytochrome P450 2D6? The role of key active-site residues in quinidine binding. *Journal of Biological Chemistry* 2005; **280**: 38617–38624.

Nandekar PP, Tumbi KM, Bansal N, Rathod VP, Labhsetwar LB, Soumya N, Singh S and Sangamwar AT. Chem-bioinformatics and in vitro approaches for candidate optimization: a case study of NSC745689 as a promising antitumor agent. *Medical Chemistry Research* 2013; **22**: 3728–3742.

Pal D and Mitra AK. MDR- and CYP3A4-mediated drug–herbal interactions. *Life Sciences* 2006; **78**: 2131–2145.

Patsalos PN and Perucca E. Clinically important drug interactions in epilepsy: general features and interactions between antiepileptic drugs. *Lancet Neurology* 2003; **2**: 347–356.

Peng CC, Glassman PA, Trilli LE and Hunter JH. Incidence and severity of potential drug–dietary supplement interactions in primary care patients: an exploratory study of 2 outpatient practices. *Archives of Internal Medicine* 2004; **164**: 630–636.

Pujala B, Rana S and Chakraborti AK. Zinc tetrafluoroborate hydrate as a mild catalyst for epoxide ring opening with amines: Scoepe and limitations of metal tetrafluoroborates and applications in the synthesis of antihypertensive drugs (*RS*)/(*R*)/(*S*)-metoprolols. *Journal of Organic Chemistry* 2011; **76**: 8768–8780.

Raju B, Ramesh M, Borkar RM, Padiya R, Banerjee SK and Srinivas R. Development and validation of liquid chromatography–mass spectrometric method for simultaneous determination of moxifloxacin and ketorolac in rat plasma: application to pharmacokinetic study. *Biomedical Chromatography* 2012; **26**: 1341–1347.

Rao Z, Ma YR, Qin HY, Wang YF, Wei YH, Zhou Y, Zhang GQ, Wang XD and Wu XA. Development of a LC-MS/MS method for simultaneous

determination of metoprolol and its metabolites, α-hydroxymetoprolol and *O*-desmethylmetoprolol, in rat plasma: application to the herb–drug interaction study of metoprolol and breviscapine. *Biomedical Chromatography* 2015; **29**: 1453–1460.

Rowland P, Blaney FE, Smyth MG, Jones JJ, Leydon VR, Oxbrow AK, Lewis CJ, Tennant MG, Modi S, Eggleston DS, Chenery RJ and Bridges AM. Crystal structure of human cytochrome P450 2D6. *Journal of Biological Chemistry* 2006; **281**: 7614–7622.

Schenkman JB and Cinti DL. Preparation of microsomes with calcium. *Methods of Enzymology* 1978; **52**: 83–89.

Scott AK, Cameron GA and Hawksworth GM. Interaction of metoprolol with lorazepam and bromazepam. *European Journal of Clinical Pharmacology* 1991; **40**: 405–409.

Sproule BA, Naranjo CA, Brenmer KE and Hassan PC. Selective serotonin reuptake inhibitors and CNS drug interactions. A critical review of the evidence. *Clinical Pharmacokinetics* 1997; **33**: 454–471.

Takemoto K, Yamazaki H, Tanaka Y, Nakajima M and Yokoi T. Catalytic activities of cytochrome P450 enzymes and UDP-glucuronosyltransferases involved in drug metabolism in rat everted sacs and intestinal microsomes. *Xenobiotica* 2003; **33**: 43–55.

Templeton IE, Thummel KE, Kharasch ED, Kunze KL, Hoffer C, Nelson WL and Isoherranen N. Contribution of itraconazole metabolites to inhibition of CYP3A4 in vivo. *Clinical Pharmacological Therapy* 2008; **83**: 77–85.

Unwalla RJ, Cross JB, Salaniwal S, Shilling AD, Leung L, Kao J and Humblet C. Using a homology model of cytochrome P450 2D6 to predict substrate site of metabolism. *Journal of Computer Aided Molecular Design* 2010; **24**: 237–256.

US Food and Drug Administration. FDA Guidance for Industry: Bioanalytical Method Validation. US Department of Health and Human Services, Food and Drug Administration, Center for Drug Evaluation and Research: Rockville, MD, 2001

US Food and Drug Administration. FDA Guidance for Industry: Drug Interaction Studies–Study Design, Data Analysis, Implications for Dosing, and Labeling Recommendations. US Department of Health and Human Services, Food and Drug Administration, Center for Drug Evaluation and Research: Rockville, MD, 2012;

Wan H and Bergstrom F. High throughput screening of drug-protein binding in drug discovery. *Journal of Liquid Chromatography and Related Technology* 2007; **30**: 681–700.

Yano JK, Wester MR, Schoch GA, Griffin KJ, Stout CD and Johnson EF. The structure of human microsomal cytochrome P450 3A4 determined by X-ray crystallography to 2.05 – a resolution. *Journal of Biological Chemistry* 2004; **279**: 38091–38094.

Yeo RK, Jamei M, Yang J, Tucker GT and Hodjegan-Rostami A. Physiologically based mechanistic modelling to predict complex drug–drug interactions involving simultaneous competitive and time-dependent enzyme inhibition by parent compound and its metabolite in both liver and gut – the effect of diltiazem on the time-course of exposure to triazolam. *European Journal of Pharmaceutical Science* 2010; **39**: 298–309.

Yeung CK, Fujioka Y, Hachad H, Levy RH and Isoherranen N. Are circulating metabolites important in drug–drug interactions?: quantitative analysis of risk prediction and inhibitory potency. *Clinical Pharmacological Therapy* 2011; **89**: 105–113.

Yoon IS, Choi MK, Kim JS, Shim CK, Chung SJ and Kim DD. Pharmacokinetics and first-pass elimination of metoprolol in rats: contribution of intestinal first-pass extraction to low bioavailability of metoprolol. *Xenobiotica* 2011; **41**: 243–251.

Yu H and Tweedie D. A perspective on the contribution of metabolites to drug–drug interaction potential: the need to consider both circulating levels and inhibition potency. *Drug Metabolism and Disposition* 2013; **41**: 536–540.

Zhang JY, Liu H, Xu HW and Shan LH. Non-enzymatic kinetic resolution of β-amino alcohols using C-12 higher carbon sugar as a chiral auxiliary. *Tetrahedron: Asymmetry* 2008; **19**: 512–517.

Zhang X, Jones DR and Hall SD. Prediction of the effect of erythromycin, diltiazem, and their metabolites, alone and in combination, on CYP3A4 inhibition. *Drug Metabolism and Disposition* 2009; **37**: 50–160.

SUPPORTING INFORMATION

Additional supporting information may be found in the online version of this article at the publisher's web site.